Heliyon 10 (2024) e23221

Contents lists available at ScienceDirect

Heliyon

journal homepage: www.cell.com/heliyon

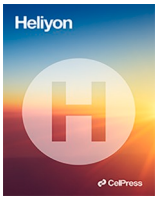

Formulation of silymarin binary and ternary solid dispersions: Characterization, simulation study and cell viability assessment against lung cancer cell line

Fai A. Alkathiri, Sarah I. Bukhari, Syed Sarim Imam *, Sultan Alshehri, Wael A. Mahdi

Department of Pharmaceutics, College of Pharmacy, King Saud University, Riyadh 11451, Saudi Arabia

ARTICLE INFO

Keywords:
Silymarin
Solid dispersion
Solubility study
Lung cancer
Cell viability

ABSTRACT

Silymarin (SL) is a water-insoluble flavonoid used in the treatment of different diseases, but its therapeutic activity is limited due to its low solubility. So, in the present study, SL solid dispersions (SDs) were developed using different carriers like Kollidone VA64 (KL), Soluplus (SP), and Poloxamer 188 (PL) by solvent evaporation (SE), microwave irradiation (MI), and freeze-drying (FD) methods. The phase solubility and saturation solubility studies were assessed to estimate the stability constant as well as the carrier effect. The dissolution studies were performed for prepared SL-SDs (binary and ternary) to select the optimum SL-SDs. The selected SL-SDs (F5, F9) were further characterized for infrared spectroscopy (IR), nuclear magnetic resonance (NMR), differential scanning calorimeter (DSC), scanning electron microscope (SEM), and X-ray diffraction (XRD). Finally, the comparative cell viability assay (lung cancer cell line) was performed to evaluate the change in activity after the formulation of SDs. The phase solubility and solubility study results displayed marked enhancements in solubility. The dissolution study findings showed significant enhancement in drug release from ternary solid dispersions (F7–F9) > ternary physical mixture (PM3) > binary solid dispersions (F1–F6) > binary physical mixture (PM1, PM2) in comparison to free SL. A greater release was observed from ternary SDs due to the addition of PL in the formulation, which had a synergistic effect on increasing the solubility. IR and NMR spectra revealed no chemical interaction between SL, KL, and PL. DSC, XRD, and SEM all confirmed the transformation of crystalline SL into amorphous SL. The cell viability assay demonstrated significantly enhanced results from ternary solid dispersion (F9) compared to free SL. Based on the study results, it can be said that SL-SDs are an alternative way to deliver drugs orally that can improve solubility and have anti-cancer activity.

1. Introduction

Drug solubility substantially impacts bioavailability, with around 70 % of recently discovered drugs showing poor solubility [1]. Amorphization is a technique for increasing the solubility of weakly water-soluble drugs, resulting in increased bioavailability. Amorphous compounds are classified as either pure drugs or solid dispersions (SDs), in which the active component is dispersed in a

* Corresponding author.
E-mail address: simam@ksu.edu.sa (S.S. Imam).

https://doi.org/10.1016/j.heliyon.2023.e23221
Received 1 October 2023; Received in revised form 28 November 2023; Accepted 29 November 2023
Available online 3 December 2023

carrier. SDs are further categorized into four types based on the carrier used: a crystalline carrier, a polymeric carrier, a carrier with surface activity, and those that use controlled release or swellable/water-insoluble polymers [2]. The amorphous form of many poorly water-soluble drugs can enhance many folds in apparent solubility and quicker dissolution [3].

SD formulations are prepared with a hydrophobic drug and a hydrophilic carrier. There were several types of carriers used to disperse the drug, such as polyvinylpyrrolidone, polyethylene glycol, hydroxypropyl methylcellulose, soluplus, kolliphore, kollidone, and poloxamer [4,5]. The different polymers used to prepare SDs displayed different physicochemical properties. So, the selection of carriers is very critical to preparing a stable formulation. The polymeric carrier must be inert and compatible with the active ingredients. The ideal characteristic of a carrier must be that it should protect the drug from recrystallization in supersaturation conditions [6]. The carrier must have a high glass transition temperature (Tg) value, which may help enhance the SDs stability at room temperature [7,8]. Recently, the use of surface-active agents as a carrier system has led to reduced interfacial tension, enhanced wettability, and the solubilization of drugs via micelle formation [4,6,9]. The use of a single polymer may not be able to form stable SDs, so the formation of ternary SDs using the drug with two carriers could mitigate the solubility and stability of the formulation. It can enhance many-fold dissolution and bioavailability compared with binary solid dispersions [10,11]. The use of two carrier systems in SDs formulation showed synergistic effects in solubilization [10,12], maintenance of the supersaturated state, reduction of molecular mobility [10], and formation of drug-polymer-polymer interactions [13,14]. The polymers used in this study are hydrophilic in nature and widely reported in the formulation of binary as well as ternary solid dispersions. Soluplus (SP) is a hydrophilic, biodegradable, biocompatible, and nano-ionic polymer having a molecular weight between 90 and 1,40,000 g/mol. It is made up of polyethylene glycol, polyvinyl acetate, and polyvinyl caprolactam [15]. Its 1-methyl-2-pyrrolidone hydrogen bond acceptor group is responsible for hydrogen bonding [5].

It has a bifunctional property (matrix polymer for solid solution and solubilizer) and is widely used in the formulation of the fourth generation of solid dispersion [16]. It has a slightly surface-active agent property and can be useful to maintain the supersaturation of poorly soluble drugs in the gastrointestinal tract [17]. Kollidone VA64 (KL) is a hydrophilic carrier made up of a blend of two monomers, N-vinylpyrrolidone and vinyl acetate, in a ratio of 6:4 [18]. It contains two hydrogen bond acceptors from the carbonyl group of the pyrrolidone ring, as well as vinyl acetate [19]. There are various advantages, like good flowability, faster extruder feeding, and extruding at 220 °C without degradation. It also has a low water content and foaming property, which reduces the risk of drug hydrolysis. It can also be used in combination with surfactants to improve the solubility of poorly soluble drugs [20,21].

Numerous reports on the usage of poloxamer (PL) in the formulation of SDs with different drugs have been published [22,23,24]. It has an amphiphilic structure as a result of having an ethylene oxide hydrophilic core and polypropylene oxide hydrophobic core blocks organized in a triblock pattern. For the solubilization of drugs that are slightly water-soluble, it aids in the formation of micelles and liquid crystalline phases with increased hydrophilicity. The drug particle is either attached to the micelle-forming polymer or solubilized within the micelle's core [25].

Silymarin (SL: Supplementary Fig. 1) is a flavonoid, which is a type of bioactive compound that has a wide range of therapeutic uses [26]. It is a lipophilic molecule that belongs to the biopharmaceutical classification system (BCS) class II drugs. It has poor solubility (50–430 μg/mL) and low bioavailability (23–47 %) due to the first-pass effect [27,28]. Despite the therapeutic benefits of SL, it is used at high doses (280–1000 mg) and has limited absorption properties [28]. To increase SL solubility and bioavailability, several oral formulation strategies [29], like solid dispersions [28,30,31], and the cyclodextrin complex [32], have been tried. Due to its low solubility and permeability, high metabolism, and fast excretion, its bioavailability is limited [33]. A solid dispersion of silymarin using D-tocopherol polyethylene glycol 1000 succinate as a carrier was prepared by the freeze-drying method. The prepared solid dispersion depicted a marked enhancement in water solubility (23-fold). The used carrier displayed a great solubilizing agent [28]. A silymarin-loaded self-emulsifying system was prepared using tween 20, HCO-50, and transcutol. The prepared system enhanced the oral bioavailability of silymarin by about 16-fold [34]. In another delivery system, solid lipid nanoparticles were prepared and evaluated for bioavailability enhancement. They have reported a 2.8-fold increase in oral bioavailability [35]. Different lipid-based formulations, like liposomes, proliposomes, and PEGylated liposomes, were developed using phospholipid and cholesterol. The developed formulations displayed high encapsulation efficiency and oral bioavailability [36–38].

Till now, there has been no literature published on silymarin solid dispersion using KL, SL, and PL as carriers. So, from the above literature, we have designed the primary objective of this study to prepare silymarin solid dispersions using various carriers. The prepared formulations were evaluated for *in-vitro* release, saturation solubility, morphological features, drug-polymer interaction, and cell viability study (lung cancer cell line, A549) to evaluate the effect of prepared solid dispersions. Finally, a molecular docking study was also performed to support the findings of the in vitro cell line evaluation.

2. Materials

Silymarin (SL, purity 99 %) was procured from Sigma Aldrich, St. Louis, Missouri, United States. Kollidone VA 64 (KL), Soluplus (SP) and Poloxamer 188 (PL) were purchased from Badische Anilin-und Sodafabrik (BASF SE), 67056 Ludwigshafen, Germany and Alfa Aesar Ward Hill, Massachusetts (MA), United States. Lung cancer cell line (A549) were obtained from the German Collection of Microorganisms and Cell Cultures (Braunschweig, Germany). Analytical grade chemicals and solvents were used in this study.

2.1. Experimental

2.1.1. Phase solubility study

The phase solubility studies for binary (SL-KL and SL-SP) and ternary (SL-KL-PL) samples were carried out according to the Higuchi-

Connors procedure [39]. A separate aqueous solution (25 mL) of KL and SL (0–6 mM) was prepared in the volumetric flask. An excess amount of SL was added to the volumetric flask. For the ternary mixture, a separate solution of KL was prepared with a fixed concentration of PL (2 %, w/w). The mixtures were agitated for 72 h at 25 °C in a thermostatic water bath (Grant Instrument Ltd., LSB18, Cambridge, United Kingdom). After completion of the study, 2 mL aliquots were withdrawn from each volumetric flask and then filtered. The filtrate was diluted further before measurement. The concentration of SL in each filtrate was measured by a UV spectrophotometer (UV 1601 PC, Shimadzu, Kyoto, Japan) at 280 nm. The phase solubility graphs were plotted between the drug and carrier concentrations. The slope of each composition was calculated graphically. The slope value of the phase solubility diagram and the free drug solubility data were added to equation (1) to calculate the apparent stability constant [40].

$$Ks = \frac{slope}{So\ (1 - slope)} \tag{1}$$

So = Solubility of pure SL.

2.2. Formulation of solid dispersion

2.2.1. Solvent evaporation technique

The binary (F1, F2) and ternary solid dispersions (F7) were made using the solvent evaporation method [10]. The detailed composition of the prepared SDs is shown in Table 1. The formulations were developed by weighing an amount of SL. The carrier (KL or SL) was dissolved in ethanol (10 ml). The solutions were sonicated for the complete solubilization of ingredients. The solutions were transferred to a round-bottom flask and fixed to the rotary evaporator equipment. The evaporation was done at 50 °C at a reduced pressure. The flask was rotated at 100 rpm, and the samples were run until the complete removal of organic solvent took place. The flask was removed and kept in the desiccator overnight for moisture removal. The samples were scraped from the flask and dried at 40 °C for 24 h. The dry product was then passed through sieve No. 80. For ternary SDs, poloxamer was added to the drug and carrier solution, and the same procedure was applied to prepare solid dispersion. For further use, the dry binary and ternary solid dispersion were preserved in desiccators containing desiccating substances in airtight vials.

2.3. Microwave irradiation technique

The binary (F3, F4) and ternary solid dispersions (F8) were prepared by the microwave irradiation method using single carriers and carrier blends [41]. The composition of prepared SDs is shown in Table 1. The free SL and carrier (KL or SP) were gently mixed, and this mixture was irradiated at 600 W for 12–15 min in a microwave oven (Samsung ME0113M1, Malaysia). One sample was placed in the beaker individually and irradiated. The samples were liquified after the irradiation treatment, and the final temperature was noted. The samples were removed and kept at room temperature to cool down. The solidified samples were pulverized to form powder and then sieved. Similarly, the ternary SD was prepared by adding PL to the binary powder mixture. After that, the same procedure was followed for irradiation, and the temperature was noted. The collected samples were stored in an airtight vial with desiccating agents for further use.

2.4. Freeze-drying technique

The different ratios of drug and carrier were used to prepare SL solid dispersions with single carriers (KL and SP) as well as carrier blends (KL and PL), as shown in Table 1. The pure SL was dissolved in methanol, and the carriers were dissolved in water [42]. Both solutions were mixed together, and the organic solvent was evaporated by keeping it in a vacuum dryer at 50 °C. The aqueous solution was collected and further kept on a thermostatic magnetic plate in the water bath. The samples were frozen in the refrigerator, and then

Table 1
Formulation composition of Silymarin solid dispersions using different methods.

Code	SDs	Method	SL (Molar)	KL (Molar)	SL (Molar)	PL (%, w/w)	Working condition
F1	Binary	SE	1	3			Solvent evaporated at 50 °C
F2	Binary	SE	1		3		Solvent evaporated at 50 °C
F3	Binary	MW	1	3			Irradiated for 14 min
F4	Binary	MW	1		3		Irradiated for 14 min
F5	Binary	FD	1	3			freeze drying at −55 °C
F6	Binary	FD	1		3		freeze drying at −55 °C
F7	Ternary	SE	1	3		2	Solvent evaporated at 50 °C
F8	Ternary	MW	1	3		2	Irradiated for 12 min
F9	Ternary	SD	1	3		2	freeze drying at −55 °C
PM1	Binary		1	3			NA
PM2	Binary		1		3		NA
PM3	Ternary		1	3		2	NA

SE: Solvent evaporation; MI: Microwave irradiation; FD: Freeze drying; PM: Physical mixture; SDs: Solid dispersion; SL: Silymarin; KL: Kollidone VA64; SL: Soluplus; PL: Poloxamer.

the samples were kept in a vacuum chamber for 24 h) for freeze drying at −55 °C (Alpha 1–2 LD Plus, Martin Christ, Germany). The dried samples were collected in a glass vial and kept in a desiccator for further characterization. The ternary SDs were prepared by adding PL to the KL solution, and then the procedure was followed as for binary SDs. Finally, the freeze-dried binary (F5–F6) and ternary solid dispersions (F9) were collected, transferred in airtight glass vials, and stored for further characterization.

2.5. Physical mixture

The binary physical mixture (PM1, PM2) and ternary physical mixture (PM3) were formed by grinding in pastel and motor in a fixed ratio, as shown in Table 1. SL: KL was physically pulverized and combined for even blending. The ternary physical mixture was prepared with the addition of PL to the binary physical mixture. The powder samples were uniformly mixed and triturated to get a homogenized product. The physical mixtures categorized as binary physical mixtures (PM1, PM2) and ternary physical mixtures (PM3) were collected for further evaluation.

2.6. Dissolution study

The free SL and prepared samples (binary physical mixture (PM1, PM2), binary solid dispersion (F1–F6), ternary physical mixture (PM3), and ternary solid dispersion (F7–F9)) were evaluated for release study. The study was performed by using the apparatus (Distek 2500; North Brunswick, NJ) at a temperature of 37 ± 0.5 °C. Equivalent to 5 mg of SL, the physical mixtures (PM1-PM3) and binary as well as ternary solid dispersions (F1–F9) were filled into empty capsules and added to the phosphate buffer with tween 80 (pH 6.8, volume 900 mL, 100 rpm) as dissolution medium. SL-containing dissolution media was collected from the flask at a fixed time (5, 10, 15, 30, 45, 60, 75, 90, and 120 min) and replaced with an equal volume to maintain a uniform release condition. The collected, released content is diluted and then filtered for analysis using a UV spectrophotometer at 288 nm [43].

2.7. Solubility study

Solubility was performed by taking an excess amount of each sample [free SL, physical mixture (PM1, PM2, PM3), binary solid dispersion (F1–F6), and ternary solid dispersion (F7–F9)]. The samples were transferred to a volumetric flask containing distilled water (25 mL). The volumetric flasks containing the aqueous dispersion of SL were shaken on a water bath shaker for 72 h. The samples were collected, diluted, and then filtered to remove the solid content. SL content was analyzed using a spectrophotometer [5].

2.8. Infrared spectroscopy

The drug-carrier interaction and formation of solid dispersion were performed by FTIR (ATR-FTIR, Bruker Alpha, Germany). The samples of free SL, KL, PL, binary physical mixture (PM1), binary solid dispersion (F1–F6), ternary physical mixture (PM3), and ternary solid dispersion (F7–F9) were scanned in the range of 4000–400 cm^{-1}. The scanned characteristic peaks of pure samples (SL, KL, and PL) were compared with the physical mixture and solid dispersions to observe the peak position and intensity [43].

2.9. Nuclear magnetic resonance

The investigation was conducted in order to assess the formation of solid dispersion using the drug (SL) and carriers (KL and PL). It is also used to evaluate the interaction between the drug and the carrier. The produced physical mixture and solid dispersions were analyzed individually to determine the distinctive changes in spectra [44,45]. Using an NMR scanner (Bruker; Software Top Spin 3.2, Switzerland), the components were scanned. The samples were prepared using deurated dimethyl sulfoxide (DMSO) as the solvent.

2.10. Scanning electron microscopy

To look at the surface features of free SL, carrier (KL), binary physical mixture (PM1), binary solid dispersion (F5), ternary physical mixture (PM3), and tertiary solid dispersion (F9) [42], a scanning electron microscope (JOEL, Tokyo, Japan) was used. The study was performed by spreading the samples over the holder. The photomicrographs of each sample were taken at 15 kV accelerating potential and low vacuum.

2.11. X-ray diffraction study

The change in drug crystallinity was assessed using an X-ray diffractometer (Ultima IV diffractometer, Rigaku, Japan). Each sample (free SL, KL, ternary physical mixture (PM3), and ternary solid dispersion (F9)) was taken and placed on the sample holder. The diffraction pattern of each sample was compared to check for changes in the diffraction angle and position. The study was performed with a scanning speed of 10°/min [46].

2.12. Differential scanning calorimetry

The free SL, carrier, binary physical mixture (PM1), binary solid dispersion (F5), ternary physical mixture (PM3), and ternary solid

dispersion (F9) were scanned using the instrument (DSC; Mettler Toledo, Parkway Columbus, OH). The samples (5 mg) were heated in a sealed aluminum pan over a temperature range of 30–300 °C. The study was performed with a supply of nitrogen, and the blank pan was kept as a reference. The thermograms of free SL and KL were compared with the thermograms of physical mixtures and solid dispersions to confirm changes in drug properties.

2.13. Cell viability study

The in vitro cell viability study was performed using the lung cancer cell line (A549) [44,47]. The different concentrations of free SL and silymarin ternary solid dispersion (F9) were prepared and treated with the developed cell lines. The samples were evaluated for in vitro efficacy, and the results were compared. The MTT assay method was applied to evaluate its efficacy. The cells were grown in 96-well plates with 15,000 cells per well in Dulbecco-modified Eagle media (10 % fetal bovine serum). To complete the process of cell growth, the cells were placed in an incubation chamber for 24 h. CO_2 (5 %) flowed continuously to support the growth. To assess cell viability, the free SL and SL-SD (F9) were added to the well. To metabolize the MTT by the living cells, the samples were incubated in an incubator for 4 h. The media was removed from each well, and then DMSO was added to dissolve the formazan. The measurement was carried out at 570 nm, with DMSO serving as a blank. The cell viability percentage was calculated for free SL and silymarin ternary solid dispersion (F9)

2.14. Simulation study

We used the X-ray crystal structure of caspase-3 (CAS329306) and 4-methyl-benzenesulfonamide (MB) from the Protein Data Bank (PDB code: 2XYG) to figure out its structure. Auto Dock Tools version 1.5.6 (La Jolla, CA, USA) were used to dock the ligands and the estrogen receptor (ER). Both the receptor and the ligands were protonated. Both the protein and the ligand atoms received the default charges and energy values. The grid box of binding affinity for each of the ligand atom kinds was generated, and autogrid was then utilized to draw its path.

2.15. Statistical analysis

The mean ± SD was used to present all the data. Tukey Kramer test and one-way analysis of variance (ANOVA) were utilized for statistical analysis. Statistical significance was considered for p values below 0.05. Graph pad prism was used to calculate statistical analysis.

3. Results

3.1. Phase solubility

It is used to determine the solubilizing ability of the carrier as well as the thermodynamic behavior between the drug and carrier. The phase solubility diagrams of binary (KL or SP) and ternary systems (KL and PL) are shown in Fig. 1. The solubility of SL was linearly enhanced with the increase in carrier concentration, showing the solubilizing power of the carrier. The apparent stability constant (Ks) value was calculated, and the data revealed higher Ks values for binary as well as ternary systems. The binary systems SL-SP and SL-KL showed stability constant values of 267 M^{-1} and 535 M^{-1}, respectively, whereas the ternary system (SL-KL - SP) depicted 1439 M^{-1}. The ternary system showed about a 2.6-fold and 5.3-fold enhancement in stability constant values compared to the binary systems of

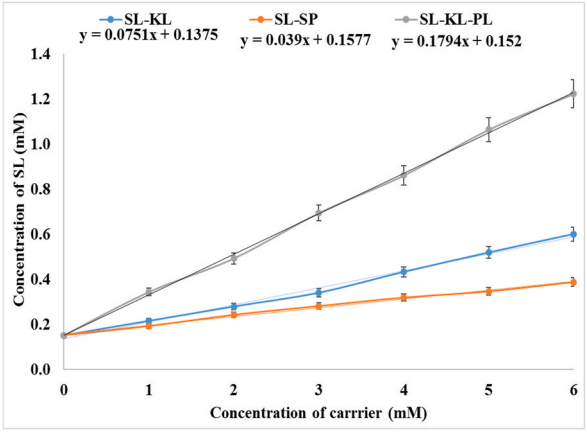

Fig. 1. Phase solubility study of Silymarin with Kollidone VA64 (SL-KL), Silymarin with Soluplus (SL- SP), Silymarin with Kollidone VA64 and poloxamer (SL-KL-PL). Data from the triplicated study are presented as mean ± SD.

SL-SP and SL-KL.

3.2. Dissolution study

It is performed to check the effect of using polymers alone as well as in blends on the SL release. The different binary and ternary physical mixtures (PM1, PM2, PM3) and binary and ternary solid dispersions (F1–F9) prepared by solvent evaporation (SE), microwave irradiation (MI), and freeze drying (FD) were evaluated. The release data was compared with the free SL and shown in Fig. 2. A significant ($p < 0.01$) difference in the release pattern was observed among all samples in 120 min. The release data shown in the pattern is as follows: F6>F5>F3>F4>F2>F1>PM2>PM1. The free SL depicted a poor release profile, with a maximum release of 32.34 ± 3.7 % in the tested 120 min. The binary physical mixture (PM1, prepared with KL) showed an enhanced (*, $p < 0.05$) drug release profile with a maximum drug release of 44.32 ± 3.7 % at the same time. The binary physical mixture (PM2, prepared with SP) showed a higher (***, $p < 0.001$) drug release of 50.12 ± 3.7 % than free SL and a non-significant (ns) difference in the release compared to the physical mixture (PM1). An increase in release was observed due to the slight reduction in crystallinity of SIL by the grinding process in the presence of polymers. In the case of binary SDs prepared with SP by solvent evaporation (F1), microwave irradiation (F3), and freeze drying (F5), there was a significant enhancement (***, $p < 0.001$) in drug release compared to free SL. The binary solid dispersions F1, F3, and F5 displayed 65.41 ± 2.9 %, 83.11 ± 4.3 %, and 90.57 ± 3.6 %, respectively, in 120 min. The other polymer used to prepare binary SDs is KL, and it showed a significantly (***, $p < 0.001$) higher drug release profile than the SDs prepared with SP (F1, F3, F5). The formulations F2, F4, and F6 showed a maximum drug release of 74.26 ± 2.8 %, 89.85 ± 3.1 %, and 99.1 ± 4.2 % in the 120-min study.

The SDs prepared with KL polymer were selected as optimized SDs, and further poloxamer (PL) was added as a ternary substance. With the addition of PL, the ternary SDs showed highly significant (***, $p < 0.001$) changes in the SL release profile (Fig. 3). All the SDs release the SL within 60 min, so the addition of PL as a ternary substance acts as a synergistic carrier with KL. The drug release profile of ternary solid dispersions (F7, F8, and F9) was compared with the ternary physical mixture (PM3). A significant (***$p < 0.001$) difference in the release profile was observed in SDs in comparison to PM3. PM3 depicted 87.83 ± 3.8 % drug release in 120 min, which is highly significantly ($p < 0.001$) enhanced than the binary physical mixture (PM1: 44.09 ± 2.8 %, PM2: 50.85 ± 3.3 %). SD prepared by SE and MI methods demonstrated a maximum drug release of 100.84 ± 3.9 % and 100.48 ± 4.2 % in 60 min. The maximum drug release was achieved in about two-fold less time than the binary SDs. In the case of SD prepared by the FD method (F9), the maximum SL release was achieved in 45 min only (100.13 ± 2.2 %). It also releases about 60 % of the drug in the initial 10 min, whereas the samples F7 and F8 release about 50–55 % of the drug.

3.3. Saturation solubility

The aqueous solubility of free SL was found to be 72.48 ± 6.8 μg/mL, which is closer to the reported value [48]. Fig. 4 displays that the solubility in water was enhanced (***$p < 0.001$) for both the binary (F1–F6) and ternary SDs (F7–F9). The binary SDs (F1, F2) prepared by SE (1167 ± 9.8 and 1101 ± 15.32 μg/mL) and MW (F3, F4) methods (1234 ± 18.7 μg/mL and 1197 ± 21.9) depicted about a 16- to 17-fold (***$p < 0.001$) increment in water solubility. But SDs (F5, F6) prepared by the FD method showed a more significant effect on SL solubility than the SDs prepared by the SE and MW methods. It showed a 22-fold (***$p < 0.001$) enhancement in solubility with a value of 1654.74 ± 18.4 μg/mL and 1561 ± 21.7 μg/mL. The formulation prepared with KL showed the highest saturation solubility of SD prepared by the freeze-drying method. The SDs prepared with the polymer KL were further modified with the addition of PL, and their saturation solubility was assessed. It revealed that the sample (F7) prepared by SE (2146 ± 19.4 μg/mL;

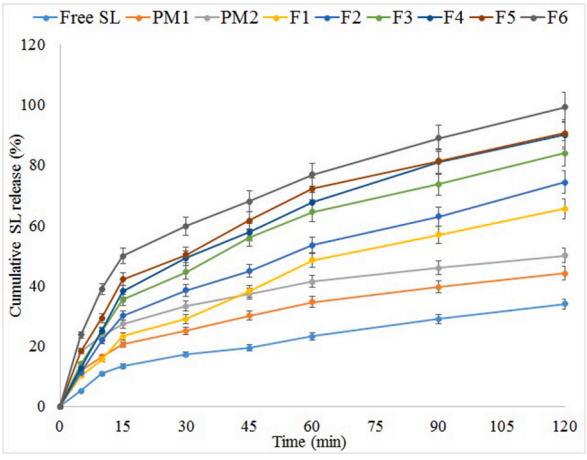

Fig. 2. Drug release of free SL, binary physical mixture (PM1, PM2) and binary solid dispersions (F1–F6). Data from the triplicated study are presented as mean ± SD.

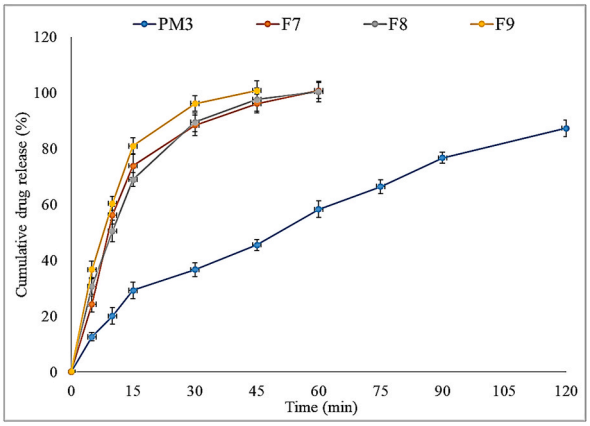

Fig. 3. Drug release profile of ternary physical mixture (PM3) and ternary solid dispersions (F7–F9). Data from the triplicated study are presented as mean ± SD.

(***$p < 0.001$), MI method (F8, 2342 ± 19.8 μg/mL; ***$p < 0.001$), and FD (F9, 3350 ± 17.1 μg/mL; (***$p < 0.001$) methods showed a about 30–45 folds increment in solubility than the free SL. Among the three SDs prepared with PL by different methods, the sample prepared by the FD method (F9) showed the maximum water solubility (1.5-fold; **$p < 0.01$) than other ternary SDs (F7 and F8).

3.4. Infra-red spectroscopy

The delineated FT-IR frequencies designated for silymarin (free SIL), carriers (KL, PL), binary and ternary physical mixtures (PM3), binary solid dispersion (F5), and ternary solid dispersion (F9) are shown in Fig. 5 and Supplementary Table 1. The illustrated peak of the free SL for the hydroxyl moieties was depicted at 3430.24 cm^{-1}, and aromatic C–H stretching vibration was observed at 2933.66 cm^{-1}. The carbonyl and C–O–C peaks were observed at 1628.60 and 1456.66 cm^{-1}, respectively. The carrier KL showed the stretching vibrations were depicted at 3432.03 and 2944.01 cm^{-1}, which may be due to the higher number of hydroxyl groups [49]. It also exhibited peaks for vinyl acetate at 1738.12 cm^{-1}. The peaks for the carbonyl group of the pyrrolidone ring were found at 1650.57 cm^{-1}. Another carrier PL, a hydroxyl stretching vibration, was depicted at 3486.79 cm^{-1}. The C–H and C–O–C stretching vibrations were observed at 2874.85 and 1096.20 cm^{-1} [50]. It revealed the similarity of the pure SL stretching vibrations of hydroxyl groups in the ternary physical mixture at 3434.02 cm^{-1}, whereas the formulations F5 and F9 depicted vibrations at 3416.23 cm^{-1} and 3414.72 cm^{-1}, respectively. This concludes that the peak for PM3 and free SL exhibited almost the same values. To draw your attention, the vibrational peak for the hydroxyl group exhibited a vast change in their peak values for formulations F5 and F9 as compared to the free SL. There was a slight difference in the peak values for C–H stretching vibration for both F5, F9, and PM3 as compared with the free SL. The peaks for the carriers (KL and PL) in formulations F5, F9, and PM3 also exhibited a slight change in their vibrational frequency.

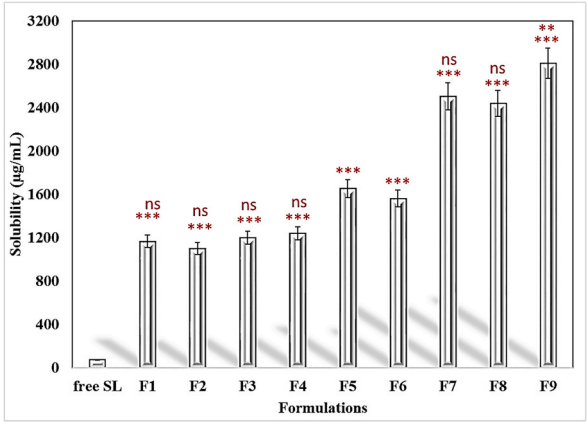

Fig. 4. Saturation solubility study results free SL, binary (F1–F6) and ternary solid dispersions (F7–F9). Data from the triplicated study are presented as mean ± SD.

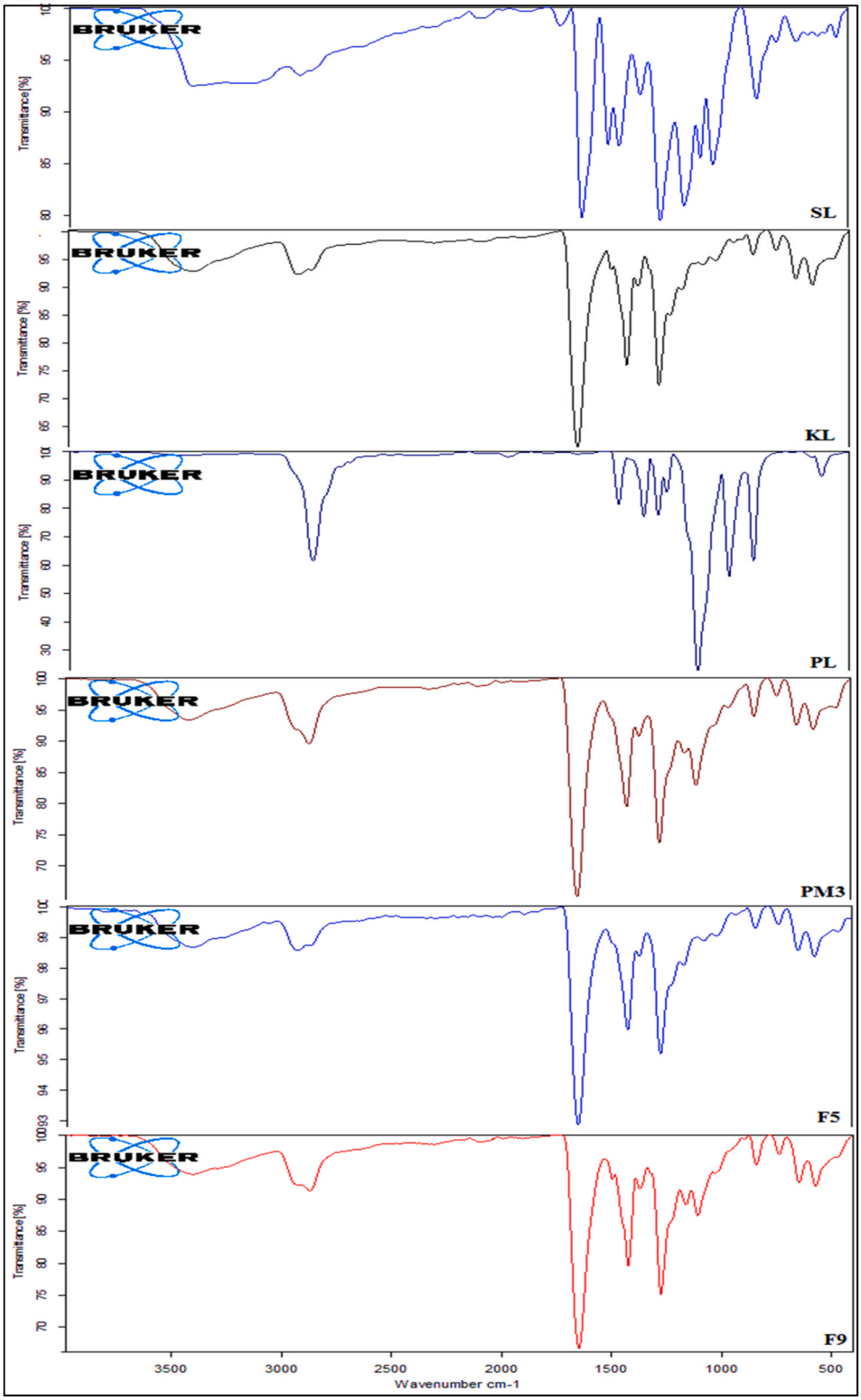

Fig. 5. IR spectroscopy study of Silymarin (SL), Kollidone VA64 (KL), Poloxamer (PL), ternary physical mixture (PM3), binary solid dispersion (F5), ternary solid dispersion (F9).

3.5. Nuclear magnetic resonance

The proton NMR spectroscopy was performed in order to strengthen our findings in concordance with the IR findings (Fig. 6 and Supplementary Table 2). The free SL showed that the proton NMR values for the deshielded hydroxyl group exhibited a definite deshielded singlet at δ 11.90 ppm for C-5, C-7, and C-20. The peaks for C-3 and C-23 hydroxyl groups were observed at δ 10.9 ppm. The multiplet peaks were depicted for aromatic hydrogens at δ 5.05–7.09 ppm. The singlet peak for the methoxy group was observed at δ 3.78 ppm for the pure drug. The samples F5, F9, and physical mixture (PM3) do not exhibit any hydroxyl group peaks for the free SL. The methoxy peaks of the free SL were observed with an insignificant change in their chemical shift values. The carrier (PL) showed the peaks at δ 3.40–3.41 ppm for F5 [51], but a drastic change in the peak values was observed in F9 and PM3, with the values at δ 3.41–3.51 ppm. The samples F5, F9, and PM3 also exhibited similar chemical shift values at δ 3.17 ppm for N–CH_2 of the pyrrolidone ring and δ 2.08 ppm for the acetate group, respectively. Apart from this, other peaks were also observed for PM3 in the range of δ 2–3 ppm. These peaks were not observed for formulation F5 and F9 spectral values.

3.6. Scanning electron microscope

The change in the surface morphology of free SL was evaluated after the addition of used carriers in the binary physical mixture (PM1), binary solid dispersion (F5), ternary physical mixture (PM3), and ternary solid dispersion (F9) shown in Fig. 7. The free SL was found in crystalline form; the particles were of elongated shape. The image of KL was found to be in an amorphous shape. The binary physical mixture (PM1) and ternary physical mixture (PM3) samples showed a slight change in the surface morphology of SL due to grinding with the carrier KL and PL. In the case of binary solid dispersion (F5) and ternary solid dispersion (F9), the images showed greater amorphization of particles.

3.7. X-ray diffraction

The study was performed to evaluate the change in crystallinity of SL after incorporating it into binary and ternary SD (Fig. 8). A significant change was observed in the peak height and peak position using the carrier KL and PL in the prepared SDs. The free SL showed a high intensity 2theta value at 22.3 (249), 24.4 (269), 38.01 (4920), and 44.28 (1785). The carrier KL showed 2 theta peaks near 12 and 22 [52]. In the physical mixture PM3, there was a slight change in peak position and peak intensity of 19.04 (282), 23.28 (206), 38.04 (4737), and 44.24 (2114) due to the grinding of free SL. It showed low-intensity peaks of drug particles, and the drug particle morphology was slightly changed into an amorphous form in the presence of carriers [53]. In the case of binary solid dispersion (F5), the drug particle peak intensity was reduced and merged with the carrier (KL) peak. But in the case of ternary solid

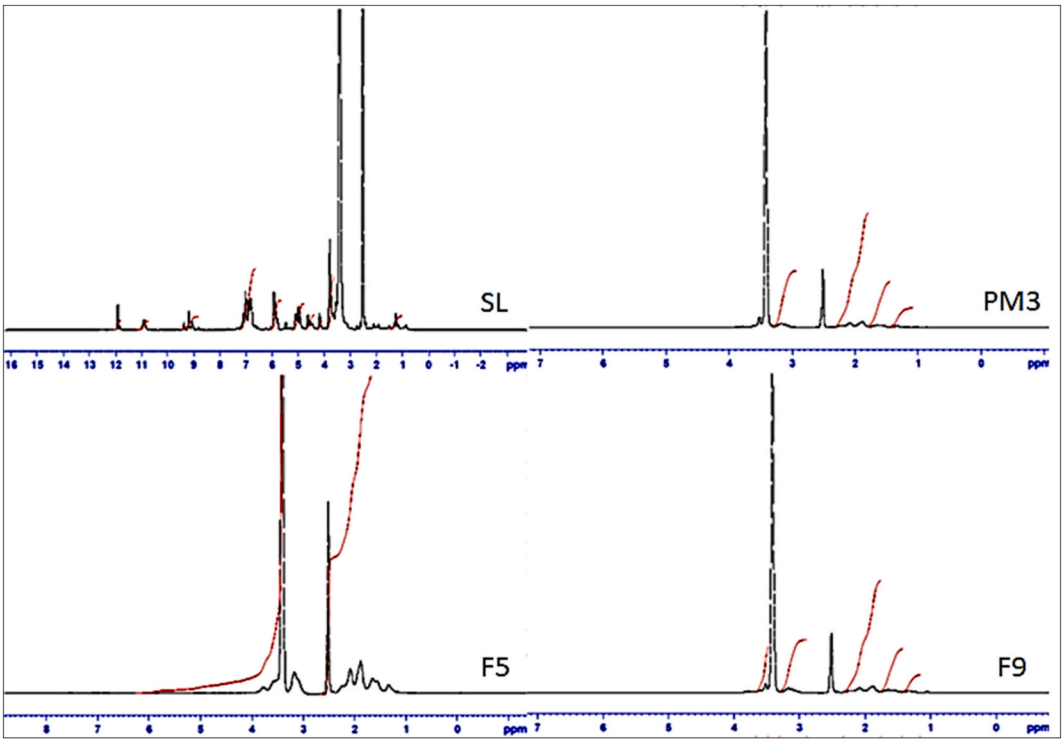

Fig. 6. NMR spectroscopy study of Silymarin (SL), ternary physical mixture (PM3), binary solid dispersion (F5), ternary solid dispersion (F9).

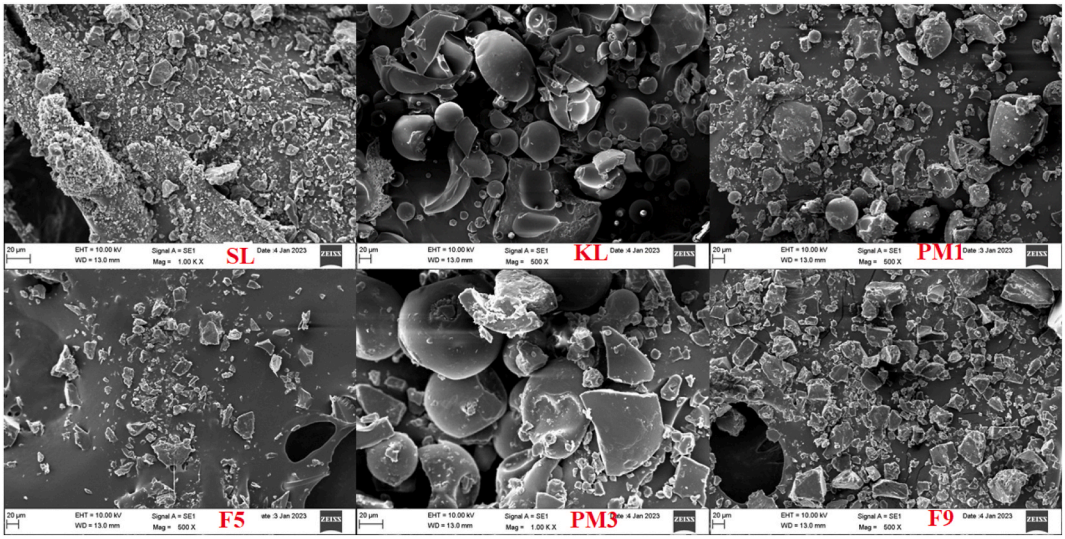

Fig. 7. SEM image of free silymarin (SL), kollidone VA64 (KL), binary physical mixture (PM1), binary solid dispersion (F5), ternary physical mixture (PM3), ternary solid dispersion (F9).

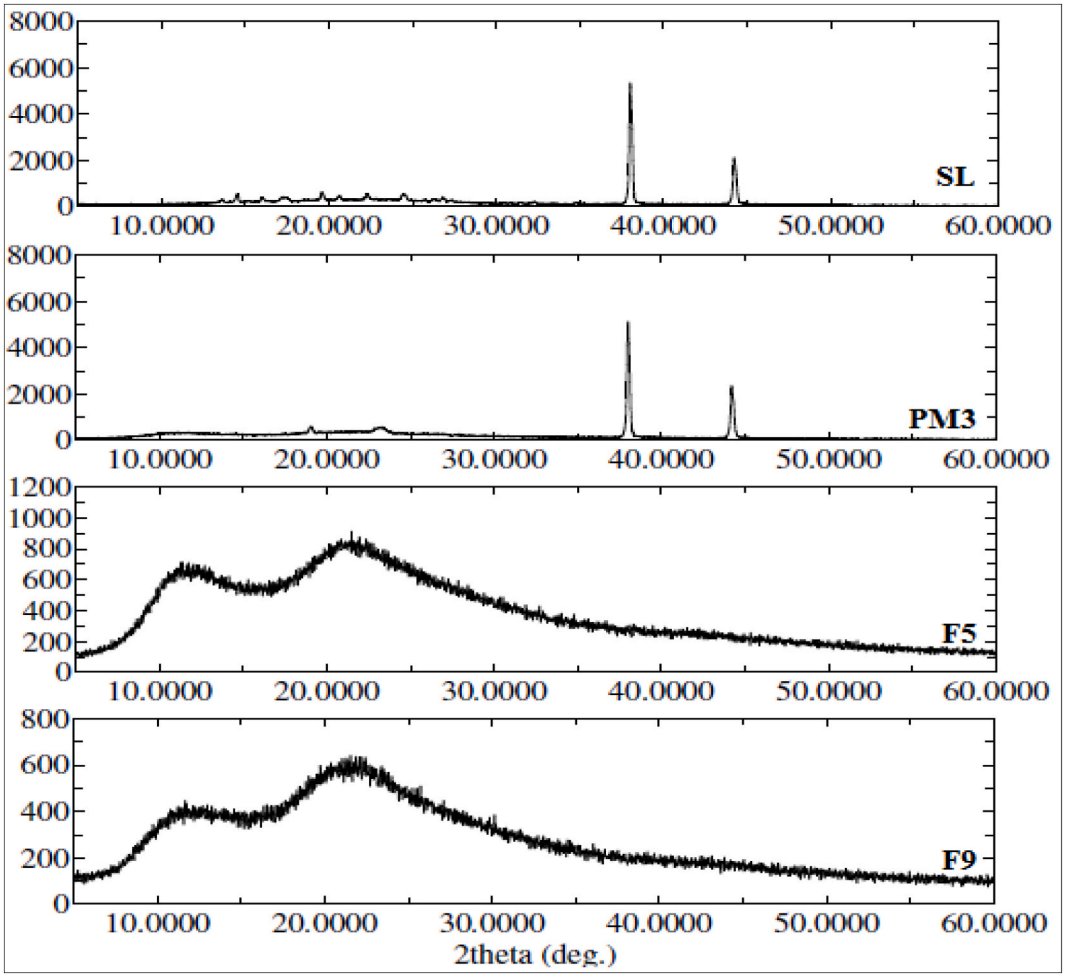

Fig. 8. XRD image of silymarin (free SL), ternary physical mixture (PM3), binary solid dispersion (F5), ternary solid dispersion (F9).

dispersion (F9), more amorphization of SL was observed.

3.8. Differential scanning calorimetry

The DSC thermograms of free silymarin (SL), kollidone (KL), poloxamer (PL), binary solid dispersion (F5), ternary physical mixture (PM3), and ternary solid dispersion (F9) are presented in Fig. 9. The thermogram of free SL demonstrated a sharp peak at 143.98 °C, which corresponds to its melting point [54]. The carriers KL and PL showed their melting points at 75.78 °C and 56.88 °C, respectively [55]. When a melting peak is broad or absent, it is apparent that the drug has been completely or partially dissolved in the carrier [52]. The binary solid dispersion (F5) and ternary physical mixture (PM3) displayed broad peaks at 74.11 °C and 53.1 °C, respectively. There is a significant change in the melting point observed for the free SL. A small peak at 163 °C was found in the sample ternary physical

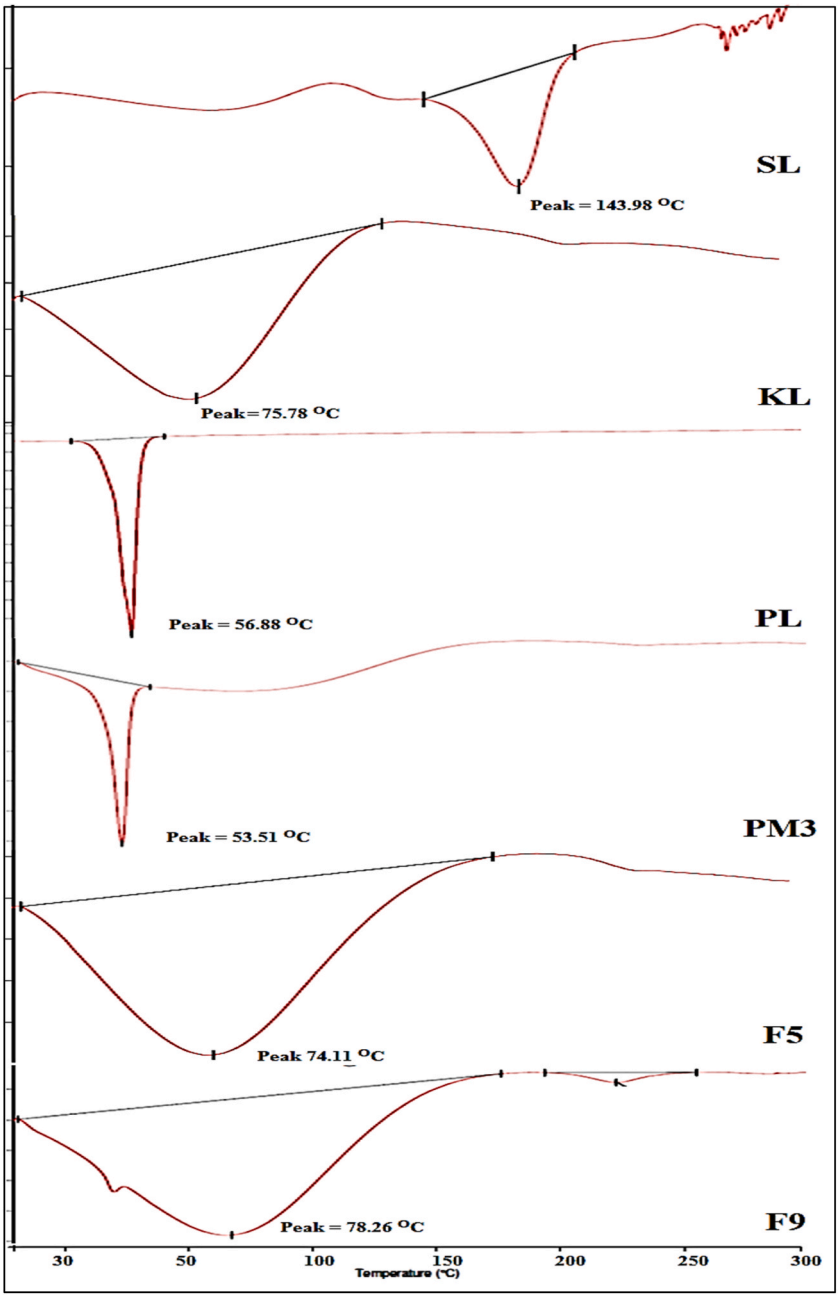

Fig. 9. DSC image of Silymarin (SL), Kollidone VA64 (KL), Poloxamer (PL), ternary physical mixture (PM3), binary solid dispersion (F5), ternary solid dispersion (F9).

mixture (PM3) due to the presence of free SL on the surface of the carrier. In the case of ternary solid dispersion (F9), no peak of SL was found due to complete solubilization in the carrier and conversion into an amorphous form [53].

3.9. Cell viability

The free SL was tested against the lung cancer cell line, and the results were compared with the prepared ternary solid dispersion (F9) as displayed in Fig. 10. The study was performed for 24 and 48 h, and then the cell viability was calculated. There was a significant variation in the result that was observed at higher concentrations and showed concentration-dependent activity. The study was performed between the 12.5 and 1000 μM concentrations, and at lower concentrations (12.5 μM and 25 μM), a non-significant (ns) variation in the activity was observed. Both samples had a lesser effect on the tested cell line. After 24 h, the ternary solid dispersion (F9) had a much stronger effect (***$p < 0.001$) than free SL after 48 h. At 24 h, it showed cell viability of 83.1 ± 7.1 % (25 μM, ns), 71.6 ± 6.3 % (50 μM, ns), 55.3 ± 4.9 % (100 μM, ***$p < 0.001$)), 41.2 ± 3.8 % (250 μM, (***$p < 0.001$), 31.8 ± 3.2 % (500 μM, (***$p < 0.001$), 22.3 ± 1.8 % (750 μM, (***$p < 0.001$) and 11.3 ± 1.8 % (1000 μM, ***$p < 0.001$). As the concentration of SL increases, cell viability also increases. The free SL showed cell viability of 86.6 ± 4.7 % (25 μM), 79.9 ± 7.1 % (50 μM), 71.3 ± 5.8 % (100 μM), 63.4 ± 9.6 % (250 μM), 57.9 ± 6.2 % (500 μM), 45.3 ± 3.2 % (750 μM), and 31.6 ± 6.2 % (1000 μM). At initial 12.5 μM and 25 μM concentrations, there was a non-significant (ns) difference in the activity observed from both free SL and ternary solid dispersion (F9). At higher concentrations (250 μM, 500 μM, 750 μM, and 1000 μM), a significant (***$p < 0.001$) enhancement in the cell viability was observed (1.4-fold, 1.8-fold, 2.1-fold, and 2.6-fold), respectively. The same samples were also evaluated at 48 h, and no significant changes in cell viability were observed. The prepared ternary solid dispersion (F9) showed cell viability of 87.1 ± 5.9 % (25 μM), 76.6 ± 4.8 % (50 μM), 63.3 ± 5.1 % (100 μM), 55.2 ± 3.9 % (250 μM), 36.5 ± 6.1 % (500 μM), 28.3 ± 3.2 % (750 μM), and 19.3 ± 2.7 % (1000 μM). There was a non-significant (ns) difference in the activity observed at 48 h compared to 24 h, but significantly (***$p < 0.001$) better than the free SL at 48 h. In the case of free SL, slightly better activity was found at 48 h than at 24 h. The different concentrations of 25 μM (87.1 ± 8.1 %), 50 μM (74.2 ± 9.4 %), 100 μM (68.3 ± 6.7 %), 250 μM (58.4 ± 6.2 %), 500 μM (51.9 ± 7.2 %), 750 μM (37.3 ± 5.3 %), and 1000 μM (25.6 ± 3.8 %) From the results, it was observed that the free SL displayed enhanced (**$p < 0.01$) activity at 48 h rather than 24 h. Whereas, ternary solid dispersion (F9) demonstrated significantly (***$p < 0.001$) better results at 24 h than at 48 h. The free SL showed the maximum effect at 1000 μM concentration at both time points, whereas the ternary solid dispersion depicted similar activity at 500 μM concentration. It was seen that ternary solid dispersion increased activity by 1.9 times (**$p < 0.01$) at the highest concentration of 1000 μM. The IC_{50} values of both samples were calculated at both time points, i.e., 24 h and 48 h. At 24 h of the treatment, the IC_{50} of F9 and free SL were calculated and found to be 171.45 ± 5.2 μM and 678.7 ± 8.5 μg/mL, respectively. After 48 h of treatment, the IC_{50} values of free SL and F9 were found to be 321.4 ± 9.4 μg/mL and 548.9 ± 12.7 μg/mL, respectively. The IC_{50} value was found to be 3.95 folds (24 h) and 1.7 folds (48 h) less (***$p < 0.001$) than the free SL. The value of IC_{50} was also found to be time-dependent.

3.10. Simulation study

As per the in vitro study result, the molecular docking was cast off to manifest silymarin (flavolignans) interaction with caspase-3 receptors by inhibiting ERά. The docked confirmation of SL and MB with the caspase-3 receptor can be visualized (Fig. 11A). The binding affinity score of pure SL was found to be −5.03 kcal/mol as compared to the ligand MB, which exhibited a binding score of −4.52 kcal/mol at the receptor. SL has the potential to bind amino acid residues from receptors since this compound has three hydrophobic regions: two hydrogen bond receptors (red) and one hydrogen bond donor (green). Further, SL formed three hydrogen bonds with the amino acid residue Ala162 having bond lengths of 2.045, 2.161, and 2.106 Å, whereas MB formed only one hydrogen

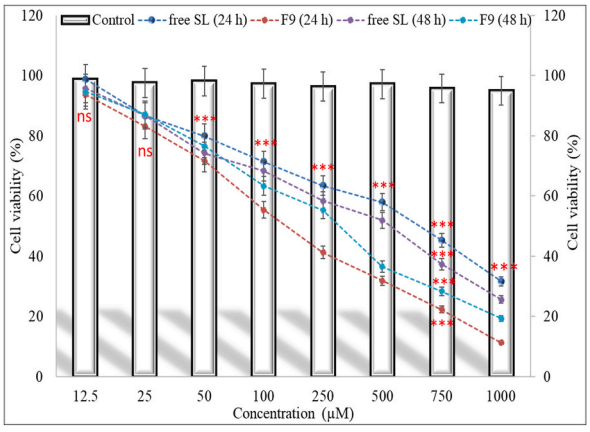

Fig. 10. Cell viability study results of free SL and ternary solid dispersion (F9) at 24 h and 48 h against lung cancer cell line (A549). Data from the triplicated study are presented as mean ± SD.

bond with Arg 164 having a bond length of 1.98 Å, respectively (Fig. 11B and Supplementary Table 3).

4. Discussion

In the current study, silymarin solid dispersions were prepared using the Kollidone VA64, Soluplus, and Poloxamer as carriers. The formulations were prepared by microwave irradiation, solvent evaporation, and freeze-drying methods. The phase solubility was performed for binary as well as ternary systems. The binary system depicted the higher stability constant, but the addition of a ternary substance (poloxamer) showed a significant (***$p < 0.001$) effect on the stability constant value. The graph was found to be AL-type, with a linear increase in carrier leading to an increase in the solubility of the drug. The higher stability constant value leads to greater sample stability. This result suggests that the carrier has a significant effect on the solubility enhancement. The in vitro drug release of the prepared SIL-SDs was performed. The binary and ternary SDs showed a significant enhancement in drug release compared to the free SL. The method of preparation also played an important role in drug release enhancement. The highly significant drug release (***, $p < 0.001$) was found in the formulation prepared by the freeze drying method due to the higher amorphization of SL achieved than other methods. There are many other reasons for higher drug release from polymer KL-based binary SDs than SP-used SDs. The higher solubility of SL in the SD formulations is due to the particle size reduction, greater wettability, and conversion to amorphous form from crystalline form [6,56]. This increase in drug release from the polymer KL may be attributed to the adsorption of drug particles, which prevents the development of drug particle size [5]. The formation of intermolecular bonds, particularly hydrogen bonds between the carbonyl functional group of pyrrolidone and vinyl acetate, may also play an important role [4]. The addition of surfactant (PL) to the SD formulation lowers the level of supersaturation, reducing drug precipitation while enhancing drug dissolution [42]. It prevents nucleation as well as thermodynamic crystal development, and it serves as both an amphiphilic surfactant and a polymeric carrier [57]. It helps to create micelles and incorporate hydrophobic drugs into the micellar core [6,58,59], leading to enhanced drug solubility. The IR study results show that there is no chemical interaction between the drug and the carrier. To make our investigation more prominent, we have performed proton NMR spectroscopy. Hence, with the above findings, it can be concluded that the formation of a stable solid dispersion takes place with free SL and carriers. The SEM study depicted that the formed particles were amorphous and irregular in shape. The presence of carrier blends (KL and PL) and the method of preparation (freeze drying) converted the particles into an amorphous shape. From the results, we can conclude that there is a greater conversion of amorphous shapes in solid dispersions, and these findings were supported by the solubility study and dissolution data [55]. In the case of the XRD study, the characteristic peak of SL was completely diminished due to higher wettability and particle size reduction. The used carriers (KL and PL) exhibited complete transformation of the drug into the amorphous form. It also suggests the formation of stable ternary solid dispersion through van der Waals interactions and/or hydrogen bonding between SL, KL, and PL. Silymarin and its formulations were evaluated against different cancer cell lines. The prepared silymarin solid dispersion showed higher cytotoxicity due to the quicker release of SL and higher cellular internalization into the tumor cells. The findings of this study were also supported by the findings of different silymarin studies.

Silymarin nanoparticles showed enhanced cell viability activity against breast and lung cancer cells [59]. The effect of the silymarin-Sn complex was also evaluated against the SW480 cell line [26]. It showed a reduction in cell viability by inducing cell death. It also displayed that the prepared formulation induces cell cycle arrest and the expression of apoptotic genes. The silymarin-HSA nanoplex was also evaluated against the LPS-treated cells [60]. The cells pre-treated with silymarin-HSA noncomplex recovered cell viability and decreased the ROS level and corresponding apoptosis more significantly than free silymarin. It was more potent and effective in suppressing the proliferation of lung cancer cell lines [61]. IC_{50} was also found to be low for the prepared silymarin solid dispersion (F9). It reduces the growth of cells as well as the IC_{50} values by triggering apoptosis. The molecular docking study also supported the findings of the cell line study. It showed the proposed mechanism of action through a simulation study between the drug (SL) and receptor (caspase-3). SL shows the anticancer effect of the activation of the caspase-3 receptor. An earlier study reported that flavonoid (SL) is a suitable candidate for preventing lung cancer by activating the caspase-3 activator [62]. According to the current investigation, the flavonoid SL may have the potential to be developed as an anticancer drug delivery system for the treatment of lung cancer. Further research is required to determine how SL affects other pathways, such as malignancy and a cell's capacity to invade other organs.

5. Conclusion

Silymarin-loaded binary and ternary solid dispersions (SDs) were prepared by different methods using kollidone VA64, soluplus, and poloxamer. The phase solubility and saturation solubility results showed a significant enhancement in the solubility of silymarin. The maximum drug release was achieved from the SDs prepared with Kollidone VA64 by the freeze-drying method, and further poloxamer was added to prepare ternary SDs. IR and NMR spectral analyses confirm no interaction between drug and carrier, as well as the formation of solid dispersion. DSC, SEM, and XRD results demonstrated the conversion of crystalline SL into an amorphous form, which supports the enhancement in solubility. The cell viability data showed significantly better activity from ternary SD (F9) than free SL at both time points (24 h and 48 h). The simulation study results displayed a good binding affinity score for pure SL as compared to the ligand MB at the receptor. From the study results, it has been concluded that silymarin solid dispersion is an alternative oral delivery system for solubility enhancement and in vitro anti-cancer activity.

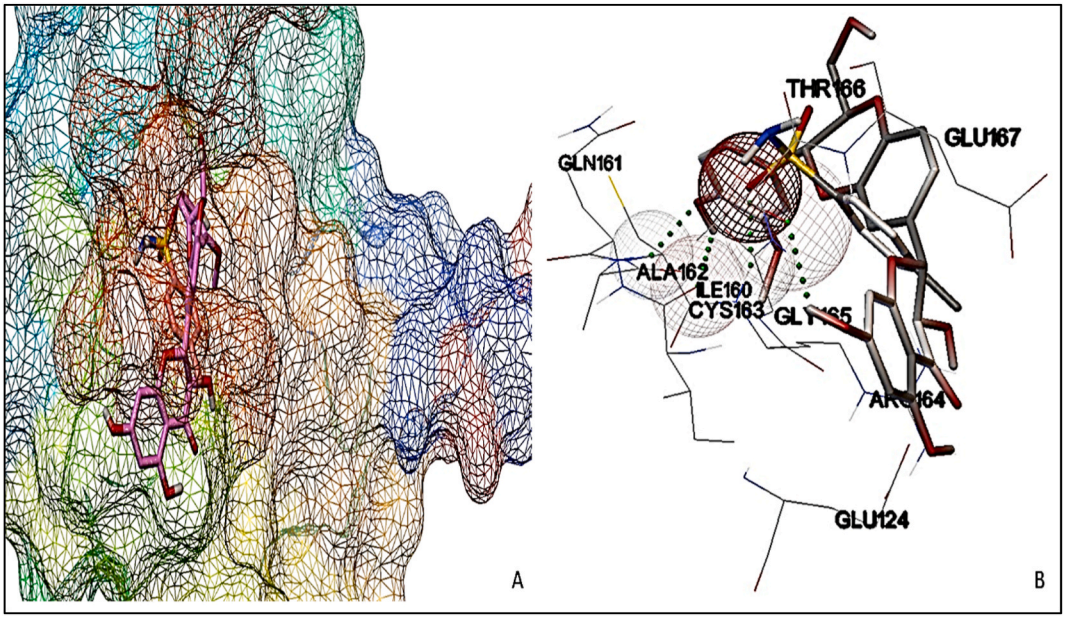

Fig. 11. A–B: (A). Docked Conformation of Silymarin and MB observed in Caspase-3 receptor (PDB ID: 2XYG); Silymarin- Magenta; MB- orange color; Receptor-rainbow color as mesh). (B). Silymarin depicting 3 Hydrogen bonds (dotted line) at 2.045, 2.161 & 2.106 Å with Ala 162 amino acid residue whereas MB formed one hydrogen bond (dotted line) at 1.98 Å with Arg 164 amino acid residue of the receptor.)

Data availability statement

Data included in the manuscript.

CRediT authorship contribution statement

Fai A. Alkathiri: Writing - original draft, Validation, Project administration, Methodology. **Sarah I. Bukhari:** Writing - review & editing, Software, Project administration, Data curation. **Syed Sarim Imam:** Methodology, Investigation, Conceptualization. **Sultan Alshehri:** Supervision, Resources, Funding acquisition. **Wael A. Mahdi:** Visualization, Supervision, Investigation, Formal analysis.

Declaration of competing interest

The authors declare that they have no known competing financial interests or personal relationships that could have appeared to influence the work reported in this paper.

Acknowledgement

The authors extend their appreciation to the Deputyship for Research and Innovation, "Ministry of Education" in Saudi Arabia for funding this research (IFKSUOR3-463-1).

Appendix A. Supplementary data

Supplementary data to this article can be found online at https://doi.org/10.1016/j.heliyon.2023.e23221.

References

[1] D.V. Bhalani, B. Nutan, A. Kumar, A.K. S Chandel, Bioavailability enhancement techniques for poorly aqueous soluble drugs and therapeutics, Biomedicines 10 (9) (2022) 2055.
[2] A.R. Tekade, J.N. Yadav, A review on solid dispersion and carriers used therein for solubility enhancement of poorly water-soluble drugs, Adv. Pharmaceut. Bull. 10 (3) (2020) 359–369.
[3] S.V. Bhujbal, B. Mitra, U. Jain, Y. Gong, A. Agrawal, S. Karki, L.S. Taylor, S. Kumar, T.Q. Zhou, Pharmaceutical amorphous solid dispersion: a review of manufacturing strategies, Acta Pharm. Sin. B 11 (8) (2021) 2505–2536.

[4] A.R. Nair, Y.D. Lakshman, V.S.K. Anand, K.S.N. Sree, K. Bhat, S.J. Dengale, Overview of extensively employed polymeric carriers in solid dispersion technology, AAPS PharmSciTech 21 (2020) 309.
[5] A. Akram, W.A. Irfan, A. Abualsunun, D.M. Bukhary, M. Alissa, How to improve solubility and dissolution of irbesartan by fabricating ternary solid dispersions: optimization and in-vitro characterization, Pharmaceutics 14 (14) (2022) 2264.
[6] R. Bajracharya, J.G. Song, S.H. Lee, S.H. Jeong, H.K. Han, Enhanced oral bioavailability of mt-102, a new anti-inflammatory agent, via a ternary solid dispersion formulation, Pharmaceutics 14 (14) (2022) 1510.
[7] S.J. Dengale, H. Grohganz, T. Rades, K. Lobmann, Recent advances in co-amorphous drug formulations, Adv. Drug Deliv. Rev. 100 (2016) 116–125.
[8] D.Q. Craig, P.G. Royall, V.L. Kett, M.K. Hopton, The relevance of the amorphous state to pharmaceutical dosage forms: glassy drugs and freeze-dried systems, Int. J. Pharm. 179 (1999) 179–207.
[9] M. Linn, E.M. Collnot, D. Djuric, K. Hempel, E. Fabian, K. Kolter, C.M. Lehr, Soluplus® as an effective absorption enhancer of poorly soluble drugs in vitro and in vivo, Eur. J. Pharmaceut. Sci. 45 (2012) 336–343.
[10] X. Shi, T. Xu, W. Huang, B. Fan, X. Sheng, Stability and bioavailability enhancement of telmisartan ternary solid dispersions: the synergistic effect of polymers and drug-polymer(s) interactions, AAPS PharmSciTech 20 (2019) 143.
[11] X. Sheng, J. Tang, J. Bao, X. Shi, W. Su W, Enhancement of in vitro dissolution and in vivo performance/oral absorption of FEB poloxamer-TPGS solid dispersion, J. Drug Deliv. Sci. Technol. 46 (2018) 408–415.
[12] S. Wairkar, R. Gaud, N. Jadhav, Enhanced dissolution and bioavailability of Nateglinide by microenvironmental pH regulated ternary solid dispersion: in-vitro and in-vivo evaluation, J. Pharm. Pharmacol. 69 (9) (2017) 1099–1109.
[13] Y. Song, X. Yang, X. Chen, H. Nie, S. Byrn, J.W. Lubach, Investigation of drug-excipient interactions in lapatinib amorphous solid dispersions using solid-state NMR spectroscopy, Mol. Pharm. 12 (3) (2015) 857–866.
[14] H. Ueda, W. Wu, K. Lobmann, H. Grohganz, A. Mullertz, T. Rades, Application of a salt coformer in a co-amorphous drug system dramatically enhances the glass transition temperature: a case study of the ternary system carbamazepine, citric acid, and l-arginine, Mol. Pharm. 15 (5) (2018) 2036–2044.
[15] K.T. Ayyub, K. Moravkar, M. Maniruzzaman, P. Amin, Effect of melt extrudability and melt binding efficiency of polyvinyl caprolactam polyvinyl acetate polyethylene glycol graft copolymer (Soluplus®) on release pattern of hydrophilic and high dose drugs, Mater. Sci. Eng. C 99 (2019) 563–574.
[16] Z.K. Nagy, A. Balogh, B. Vajna, A. Farkas, G. Patyi, A. Kramarics, G. Marosi, Comparison of electrospun and extruded Soluplus(R)-based solid dosage forms of improved dissolution, J. Pharm. Sci. 101 (1) (2012) 322–332.
[17] R.N. Shamma, M. Basha, Soluplus®: a novel polymeric solubilizer for optimization of Carvedilol solid dispersions: formulation design and effect of method of preparation, Powder Technol. 237 (2013) 406–414.
[18] D. Strojewski, A. Krupa, Kollidon®VA 64 and Soluplus® as modern polymeric carriers for amorphous solid dispersions, Polim. W. Med. 52 (2022) 17–27.
[19] L. Dong, Y. Mai, Q. Liu, W. Zhang, J. Yang, Mechanism and improved dissolution of glycyrrhetinic acid solid dispersion by alkalizers, Pharmaceutics 12 (2020) 82.
[20] W. Wang, Q. Kang, N. Liu, Q. Zhang, Y. Zhang, H. Li, B. Zhao, Y. Chen, Y. Lan, Q. Ma, Q. Wu, Enhanced dissolution rate and oral bioavailability of ginkgo biloba extract by preparing solid dispersion via hot-melt extrusion, Fitoterapia 102 (2015) 189–197.
[21] J.M. Vasoya, H.H. Desai, S.G. Gumaste, J. Tillotson, D. Kelemen, D.M. Dalrymple, A.T.M. Serajuddin, Development of solid dispersion by hot melt extrusion using mixtures of polyoxylglycerides with polymers as carriers for increasing dissolution rate of a poorly soluble drug model, J. Pharmaceut. Sci. 108 (2) (2019) 888–896.
[22] V.P. Pardhi, K. Jain, Impact of binary/ternary solid dispersion utilizing poloxamer 188 and TPGS to improve pharmaceutical attributes of bedaquiline fumarate, J. Drug Deliv. Sci. Technol. 62 (2021), 102349.
[23] E. Fousteris, P.A. Tarantili, E. Karavas, D. Bikiaris, Poly(vinyl pyrrolidone)–poloxamer-188 solid dispersions prepared by hot melt extrusion, J. Therm. Anal. Calorim. 113 (2013) 1037–1047.
[24] A. Sharma, C.P. Jain, Y.S. Tanwar, Preparation and characterization of solid dispersions of carvedilol with poloxamer 188, J. Chil. Chem. Soc. 58 (1) (2013) 1553–1557.
[25] T. Sankari, S. Al-Hariri, Preparation and characterization of cefuroxime axetil solid dispersions using poloxamer 188, Braz. J. Pharm. Sci. 54 (4) (2018), e17644.
[26] H. Abbasinia, M. Heshmati, M. Yousefi, N. Najjar, H. Sadeghi, Silymarin-loaded tin(IV) nanoparticles exhibit enhanced bioavailability and antiproliferative effects on colorectal cancer cells, ACS Appl. Bio Mater. 6 (9) (2023) 3768–3777.
[27] J.W. Wu, L.C. Lin, S.C. Hung, C.W. Chi, T.H. Tsai, Analysis of silibinin in rat plasma and bile for hepatobiliary excretion and oral bioavailability application, J. Pharm. Biomed. Anal. 45 (4) (2007) 635–641.
[28] I.S. Song, S.J. Nam, J.H. Jeon, S.J. Park, M.K. Choi, Enhanced bioavailability and efficacy of silymarin solid dispersion in rats with acetaminophen-induced hepatotoxicity, Pharmaceutics 13 (2021) 628.
[29] A. Di Costanzo, R. Angelico, Formulation strategies for enhancing the bioavailability of silymarin: the state of the art, Molecules 24 (11) (2019) 2155.
[30] D.Y. Lim, M. Pang, J. Lee, J. Lee, J.H. Jeon, J.H. Park, M.K. Choi, S.I. Song, Enhanced bioavailability and hepatoprotective effect of silymarin by preparing silymarin-loaded solid dispersion formulation using freeze-drying method, Arch Pharm. Res. (Seoul) 45 (2022) 743–760.
[31] Y. Xu, J. Li, B. He, T.S. Feng, L.J. Liang, X.H. Huang, In vitro dissolution testing and pharmacokinetic studies of silymarin solid dispersion after oral administration to healthy pigs, Front. Vet. Sci. 9 (2022), 815198.
[32] S. Gharbia, C. Balta, H. Herman, M. Rosu, J. Váradi, I. Bácskay, M. Vecsernyés, S. Gyongyosi S, F. Fenyvesi, S.N. Voicu, M.S. Stan, R.E. Cristian, A. Dinischiotu, A. Hermenean, Enhancement of silymarin anti-fibrotic effects by complexation with hydroxypropyl (HP βCD) and randomly methylated (Ram-β) cyclodextrins in a mouse model of liver fibrosis, Front. Pharmacol. 9 (2018) 883.
[33] H. Hwang du, Y.I. Kim, K.H. Cho, B.K. Poudel, J.Y. Choi, D.W. Kim, Y.J. Shin, O.N. Bae, A.M. Yousaf, C.S. Yong, J.O. Kim, H.G. Choi, A novel solid dispersion system for natural product-loaded medicine: silymarin-loaded solid dispersion with enhanced oral bioavailability and hepatoprotective activity, J. Microencapsul. 31 (7) (2014) 619–626.
[34] J.S. Woo, T.S. Kim, J.H. Park, S.C. Chi, Formulation and biopharmaceutical evaluation of silymarin using SMEDDS, Arch Pharm. Res. (Seoul) 30 (2007) 82–89.
[35] J. He, S.X. Hou, W.G. Lu, L. Zhu, J.F. Feng, Preparation, pharmacokinetics and body distribution of silymarin-loaded solid lipid nanoparticles after oral administration, J. Biomed. Nanotechnol. 3 (2007) 195–202.
[36] A. Di Costanzo, R. Angelico, Formulation strategies for enhancing the bioavailability of silymarin: the state of the art, Molecules 24 (2019) 2155.
[37] Y.Y. Xiao, Y.M. Song, Z.P. Chen, Q.N. Ping, Preparation of silymarin proliposome: a new way to increase oral bioavailability of silymarin in beagle dogs, Int. J. Pharm. 319 (2006) 162–168.
[38] C. Chu, S.S. Tong, Y. Xu, L. Wang, M. Fu, Y.R. Ge, J.N. Yu, X.M. Xu, Proliposomes for oral delivery of dehydrosilymarin: preparation and evaluation in vitro and in vivo, Acta Pharmacol. Sin. 32 (2011) 973–980.
[39] T. Higuchi, K.A. Connors, Phase solubility techniques, Advanced Analytical Chemistry of Instrumentation 4 (1965) 117–212.
[40] A.P. Sherje, V. Kulkarni, M. Murahari, U.Y. Nayak, P. Bhat, V. Suvarna, B. Dravyakar, Inclusion complexation of etodolac with hydroxypropyl-betacyclodextrin and auxiliary agents: formulation characterization and molecular modeling studies, Mol. Pharm. 14 (2014) 1231–1242.
[41] M. Moneghini, N. De Zordi, M. Grassi, G. Zingone, Sustained-release solid dispersions of ibuprofen prepared by microwave irradiation, J. Drug Deliv. Sci. Technol. 18 (5) (2008) 327–333.
[42] V.V. Kulthe, P.D. Chaudhari, H.Y. Aboul-Enein, Freeze-dried amorphous dispersions for solubility enhancement of thermosensitive api having low molecular lipophilicity, Drug Res. 64 (2014) 493–498.
[43] A.E. El-Nahas, A.N. Allam, D.A. Abdelmonsif, A.H. El-Kame, Silymarin-loaded eudragit nanoparticles: formulation, characterization, and hepatoprotective and toxicity evaluation, AAPS PharmSciTech 18 (8) (2017).
[44] S.S. Imam, S. Alshehri, M.A. Altamimi, W.A. Mahdi, W. Qamar, Formulation of silymarin-β cyclodextrin-TPGS inclusion complex: physicochemical characterization, molecular docking, and cell viability assessment against breast cancer cell lines, ACS Omega 8 (38) (2023) 34898–34907.

[45] M. Patel, R. Hirlekar, Multicomponent cyclodextrin system for improvement of solubility and dissolution rate of poorly water soluble drug, Asian J. Pharm. Sci. 14 (1) (2019) 104–115.
[46] G. Chawla, A.K. Bansal, A comparative assessment of solubility advantage from glassy and crystalline forms of a water-insoluble drug, Eur. J. Pharmaceut. Sci. 32 (2007) 45–57.
[47] S.S. Imam, S. Alshehri, W.A. Mahdi, A.M. Alotaibi, M.H. Alhwaifi, A. Hussain, M.A. Altamimi, W. Qamar, Formulation of multicomponent chrysin-hydroxy propyl β cyclodextrin-poloxamer inclusion complex using spray dry method: physicochemical characterization to cell viability assessment, Pharmaceuticals 15 (12) (2022) 1525.
[48] https://pubchem.ncbi.nlm.nih.gov/compound/silymarin.
[49] R.G. Shriram, A. Moin, H.F. Alotaibi, E.S. Khafagy, A. Al Saqr, A.S. Abu Lila, R.N. Charyulu, Phytosomes as a plausible nano-delivery system for enhanced oral bioavailability and improved hepatoprotective activity of silymarin, Pharmaceuticals 15 (2022) 790.
[50] J.N. Pawar, R.T. Shete, A.B. Gangurde, K.K. Moravkar, S.D. Javeer, D.R. Jaiswar, P.D. Amin, Development of amorphous dispersions of artemether with hydrophilic polymers via spray drying: physicochemical and in silico studies, Asian J. Pharm. Sci. 11 (2016) 385–395.
[51] M. Ossama, R.M. Hathout, D.A. Attia, N.D. Mortada, Augmented cytotoxicity using the physical adsorption of Poloxamer 188 on allicin-loaded gelatin nanoparticles, J. Pharm. Pharmacol. 73 (5) (2021) 664–672.
[52] S.S. Gupta, N. Solanki, A.T.M. Serajuddin, Investigation of thermal and viscoelastic properties of polymers relevant to hot melt extrusion, IV: affinisol™ HPMC HME polymers, AAPS PharmSciTech 17 (2015) 148–157.
[53] M.A. Altamimi, E.M. Elzayat, W. Qamar, S.M. Alshehri, A.Y. Sherif, N. Haq, F. Shakeel, Evaluation of the bioavailability of hydrocortisone when prepared as solid dispersion, Saudi Pharmaceut. J. 27 (2019) 629–636.
[54] W.A. Mahdi, M.M. Alanazi, S.S. Imam, S. Alshehri, A. Hussain, M.A. Altamimi, S.S. Alhudaithi, Formulation of multicomponent inclusion complex of cyclodextrin-amino acid with Chrysin: physicochemical characterization, cell viability and apoptosis assessment in human primary glioblastoma cell line, Int. J. Pharm. X. 6 (2023), 100211.
[55] N.M. Sheta, S.A. Boshra, M.A. Mamdouh, K.M. Abdel-Haleem, Design and optimization of silymarin loaded in lyophilized fast melt tablets to attenuate lung toxicity induced via $HgCl_2$ in rats, Drug Deliv. 29 (1) (2022) 1299–1311.
[56] T. Vasconcelos, F. Prezotti, F. Araujo, C. Lopes, A. Loureiro, S. Marques, B. Sarmento, Third-generation solid dispersion combining soluplus and poloxamer 407 enhances the oral bioavailability of resveratrol, Int. J. Pharm. 595 (2021), 120245.
[57] N.A. Kim, H.K. Oh, J.C. Lee, Y.H. Choi, S.H. Jeong, Comparison of solubility enhancement by solid dispersion and micronized butein and its correlation with in vivo study, J. Pharm. Investig. 51 (2021) 53–60.
[58] R. Bajracharya, S.H. Lee, J.G. Song, M. Kim, K. Lee, H.K. Han, Development of a ternary solid dispersion formulation of LW6 to improve the in vivo activity as a BCRP Inhibitor: preparation and in vitro/in vivo characterization, Pharmaceutics 11 (2019) 206.
[59] C.V. Sezer, An in vitro assessment of the cytotoxic and apoptotic potency of silymarin and silymarin loaded solid lipid nanoparticles on lung and breast cancer cells, Pakistan J. Zool. 53 (2021) 1407–1415.
[60] M.J. Sohrabi, A.R. Dehpour, F. Attar, A. Hasan, N.M. Sadeghi, A.A. Meratan, F.M. Aziz, A. Salihi, M.S. Shekha, K. Akhtari, K. Shahpasand, S.M.M. Hojjati, M. Sharifi, A.A. Saboury, S.M. Rezayat, S.E. Mousavi, M. Falahati, Silymarin-albumin nanoplex: preparation and its potential application as an antioxidant in nervous system in vitro and in vivo, Int. J. Pharm. 572 (2019), 118824.
[61] P. Patel, M. Raval, V. Airao, V. Bhatt, P. Shah, Silibinin loaded inhalable solid lipid nanoparticles for lung targeting, J. Microencapsul. 39 (1) (2022) 1–24.
[62] K.Y. Christensen, A. Naidu, M.E. Parent, J. Pintos, M. Abrahamowicz, J. Siemiatycki, A. Koushik, The risk of lung cancer related to dietary intake of flavonoids, Nutr. Cancer 64 (2012) 964–974.